Bulgarian Chemical Communications, Volume 49, Issue I, (pp. 5 – 14) 2017

Molecular modelling of 2-iminothiazoles as insecticidal activity

Asiye Meriç*

[*]*Anadolu University, Faculty of Pharmacy, Department of Pharmaceutical Chemistry, Yunusemre Campus, 26470-Tepebasi/Eskisehir, Turkiye*

Submitted June 1, 2017; Accepted September 1, 2017

Insecticides are used in agriculture, medicine, industry and by consumers, indoor. Insecticides are also claimed to be a major factor behind the increase in agricultural 20th century's productivity. On the other hand, modes of their action is important in understanding whether an insecticide will be toxic to unrelated species, such as fish, birds and mammals. On the other hand, molecular docking, a new way of illuminating the effect mechanisms of biologically active chemicals offer a new green chemistry field. As provided herein, although 2-iminothiazoles are designed, synthesized and tested as protein tyrosine phosphatase 1B inhibitors, cannabinoid receptor ligands, pifithrin-α p53 inactivators, etc. there is not any remarkably record on their insecticidal docking study. Present work introduce the molecular modelling and mapping of active site of previously synthesized by us insecticidal 2-iminothiazole derivatives, by using classical docking techniques *i.e.* MOE, etc. and discuss their result.

Key words: molecular modelling; docking; insecticide; 2-iminothiazole; acetyl CoA carboxylase

1. INTRODUCTION

Insecticides are essential tools for preventing or minimizing insect damage to, and significantly increasing the quality and quantity of crops, as well as for improving the quality of life for humans, domestic animals and livestock. There are currently more than 20 different mechanisms, or modes of action, by which various commercial insecticides control insects by disrupting specific vital biological processes, but not all of these can be used against any particular pest insect. Despite the best efforts of the entire crop protection industry, a new insecticide mode of action comes to market only every 5 or 10 years, the last being in 2007 **[1]**.

Neonicotinoid insecticides, i.e. imidacloprid (IMI) and clothianidin (CTD), which act on nicotinic acetilcholine receptors (nAChRs), yet the molecular basis of such action is poorly understood. The crystal structures in complex with aceylcholine binding protein from *Lymnaea stagnalis* (Ls-AChBP) which are deposited to Protein Data Bank (PDB) suggested that the guanidine moiety of IMI and CTD stacks with Tyr185, while the nitro group of IMI but not of CTD makes a hydrogen bond with Gln55 **[2]**.

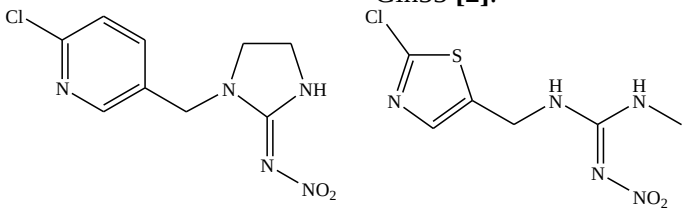

Imidacloprid (IMI) Pdb: 2ZJ**U**

Clothianidin (CTD) Pdb: 2ZJ**V**

Fig. 1. Neonicotinoid insecticides

IMI showed higher binding affinity for Ls-AChBP than that of CTD, consistent with weaker CH–p interactions in the Ls-AChBP–CTD complex than in the Ls-AChBP–IMI complex and the lack of the nitro group-Gln55 hydrogen bond in CTD. Yet, the NH at position 1 of CTD makes a hydrogen bond with the backbone carbonyl of Trp143, offering an explanation for the diverse actions of neonicotinoids on nAChRs **[2]**.

With an aim to explore the binding sites, the complementary applications of molecular docking were employed to understand the interaction between bovine serum albumin (BSA) and the organophosphate insecticides monocrotophos and phosphamidon **[3],** cf. Fig. 4.

* To whom all correspondence should be sent.
E-mail: americ@anadolu.edu.tr; asiye.meric@gmail.com

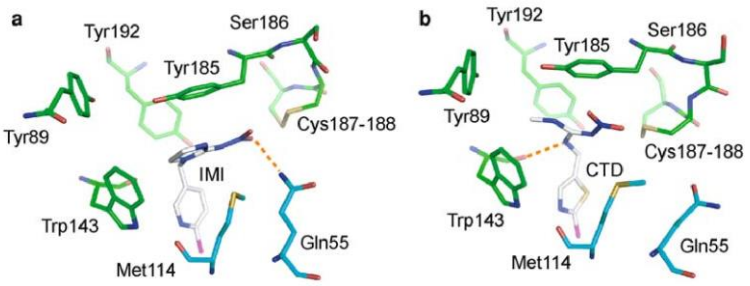

Fig. 2. Imidacloprid (IMI) and clothianidin (CTD) binding to *Lymnaea stagnalis* AChBP (Ls-AChBP). (**a)** IMI–Ls-AChBP complex. (**b)** CTD–Ls-AChBP complex **[2]**.

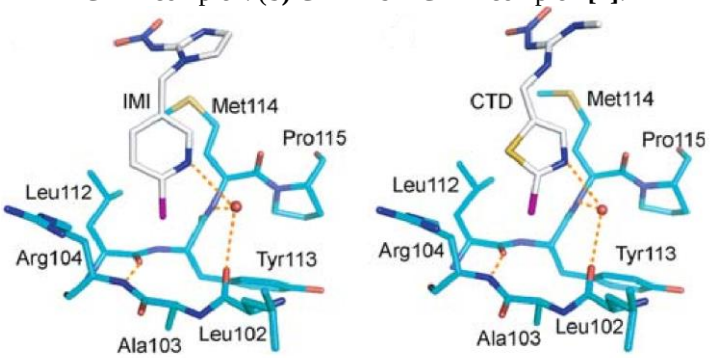

Fig. 3. Electron density maps of bound ligands and their interactions with the loop E region **[2]**.

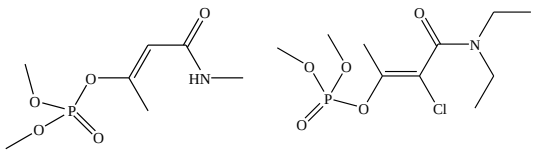

Monocrotophos Phosphamidon

Fig. 4. Organophosphate insecticides monocrotophos and phosphamidon.

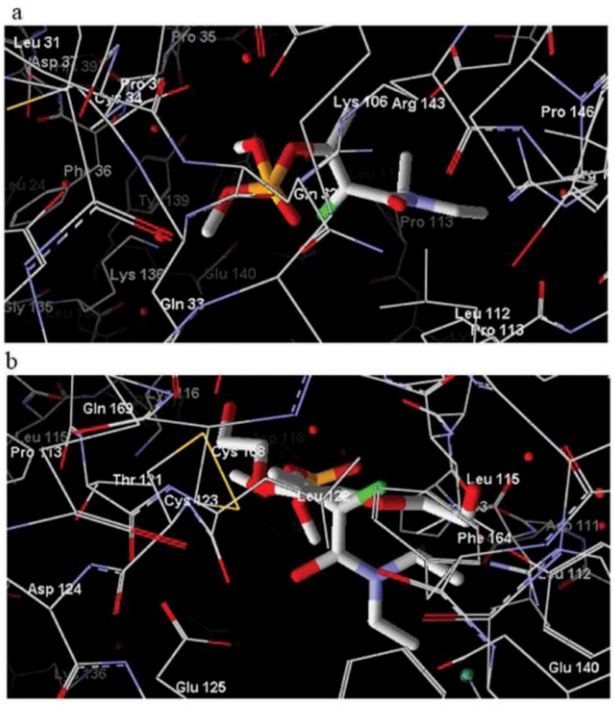

Fig. 5. The molecular docking results suggested that the insecticides bind to BSA into the hydrophobic cavity of subdomain IIA [3].

Among several classes of pesticides, carbamate compounds are widely used insecticides and acaricides. Formetanate (FMT) is one of them [4].

Laccases which are found in many plants, fungi and microorganisms are copper-containing oxidase enzymes. The latest research regarding modeling of laccase inhibition by formetanate suggested that the calculations identified Asp206 as the most relevant moiety in the interaction of FMT with the laccase enzymatic ligand binding domain. The amino acid residue Cys453 was important, because the Cys453-FMT interaction energy was not affected by the dielectric constant, although it was not a very close residue **[4]**.

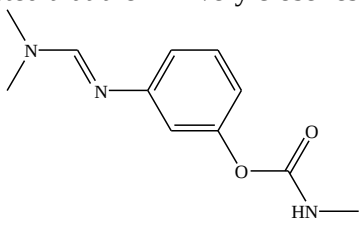

Fig. 6. Formetanate (FMT).

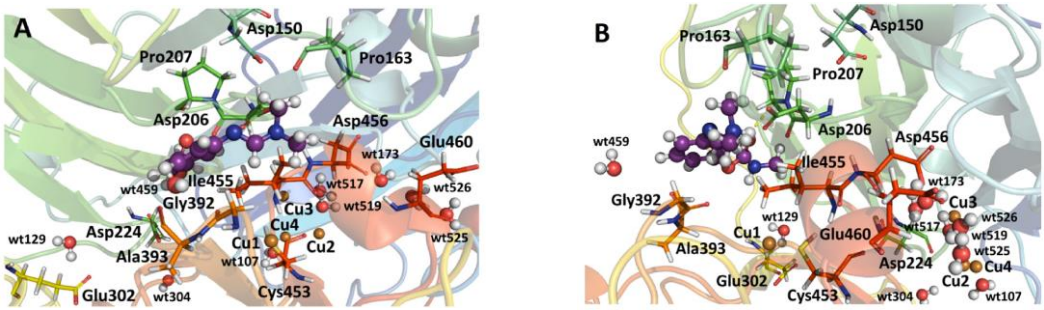

Fig. 7. Schematic representation of the binding pocket of the Lac showing the most important residues involved in the binding interaction in two different views. The only relevant residue that forms a hydrogen bond with **FMT** is **Asp206**, as shown in **B**. **Cys453** residue is important for interaction [4].

QSAR analyses of organophosphates for insecticidal activity and its *in-silico* validation using molecular docking study have been revealed that selected OP analogues from combinatorial library were docked against the generated model of AChE of *M. domestica* as receptor. The binding pockets of these ligands were observed to be very similar to that of other OPs including TCVP as reported earlier, thus hinting about the insecticidal nature of the selected OP ligands. The binding sites (**Fig. 8**) analyses reflected that four amino acid residues (Ser-235, Try-160, Trp-83, Phe-368 and His-477) were commonly present as the interacting residues with docked OP ligands. Also, the binding efficiency was elevated when other aromatic side chains (*viz*., Tyr-367, Tyr-367, *etc*.) were involved in interaction with the ligands **[5]**.

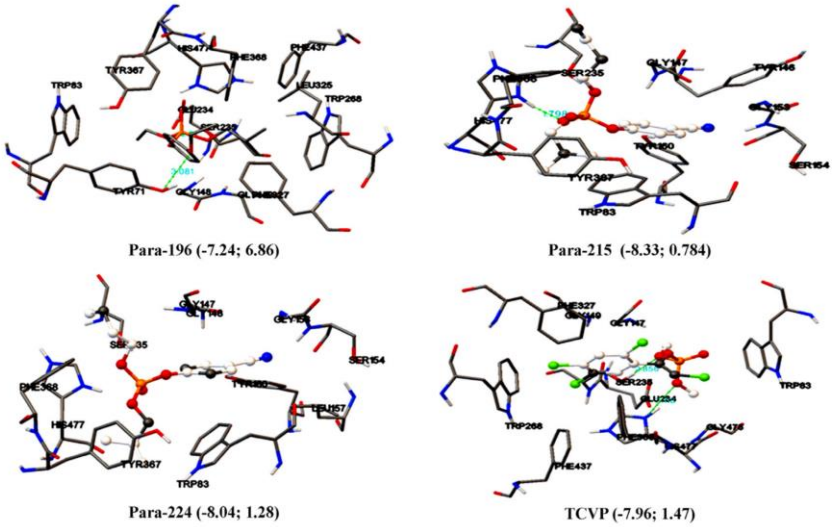

Fig. 8. The docking site of selected OP analogues of combinatorial library and Tetrachlorvinphos (**TCVP**) showing interacting residues when docked against *M. Domestica* AChE (pdb ID: **1DX4) [5]**.

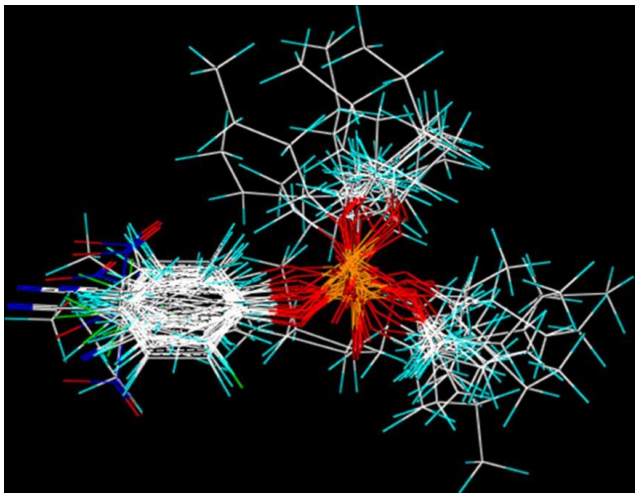

Fig. 9. Dataset compounds aligned on Molecule OP22 (maximum activity) **[5]**.

Molecular modeling of insecticides have been studied for tetronic acid derivatives via the inhibiton of acetyl-CoA carboxylase (ACCase) **[6]**.

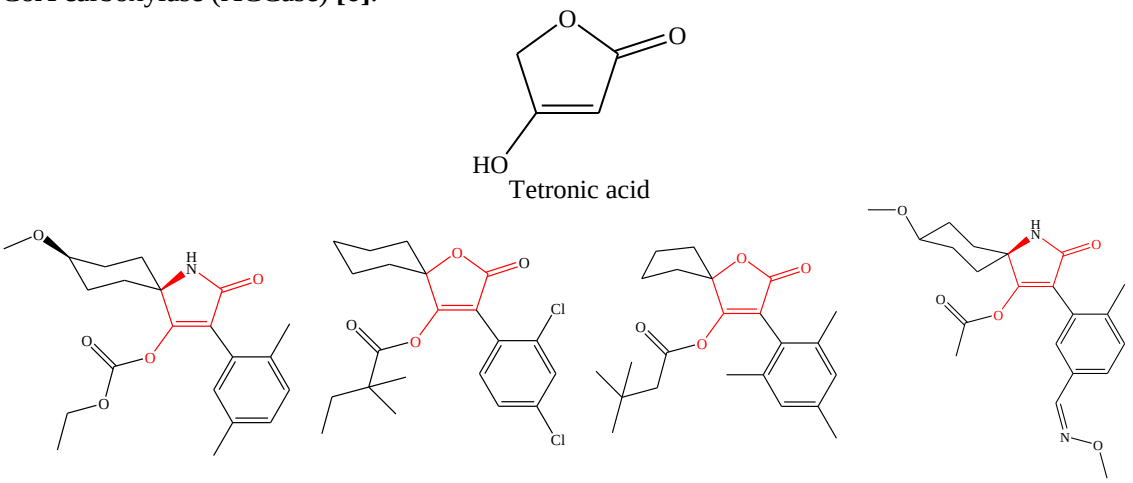

Fig. 10. The structure of representative tetronic acid derivatives and designed lead compound **[6]**.

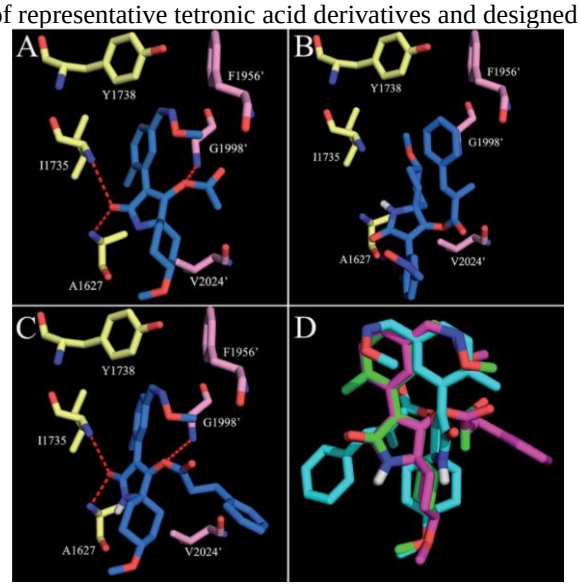

Fig. 11. Interaction mode of ACCase and active compounds 91b (**A**), 91j (**B**) and 91k (**C**) proposed by molecular docking and their molecular overlay (**D**). (pdb ID: **3PGQ) [6].**

This application relates to **thiazolylidene** containing compounds, compositions comprising such compounds, and methods of treating conditions and disorders using such compounds and compositions.

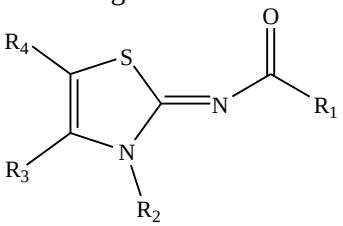

Fig. 12. Thiazolylidene compounds.

(-) – Δ^9-Tetrahydocannabinol (Δ^9-THC), the major psychoactive constituent of marijuana, exerts a broad range of effects through its interactions with two cannabinoid (CB) receptor subtypes, CB1 and CB2 **[7].**

Organophosphorus compounds (OPs) may irreversibly inhibit acetylcholinesterase (AChE), this enzyme is responsible for the hydrolysis of acetylcholine (ACh) which terminates nerve impulse transmission. A promising alternative route for OP detoxification and degradation is enzymatic catalysis. OP degrading enzymes are phosphotriesterase (PTE) (cleave different OP, breaking P-O, P-F, P-CN and Ps bonds), Human Serum Paraoxonase 1 (*Hss*PON1) (degrade substrates such as esters, lactones, oxidized phospholipids and OPs), diisopropyl fluorophosphatase (DFPase) and Human Butyrycholinesterase G117H Mutant (*Hss*BuChE) **[8]**.

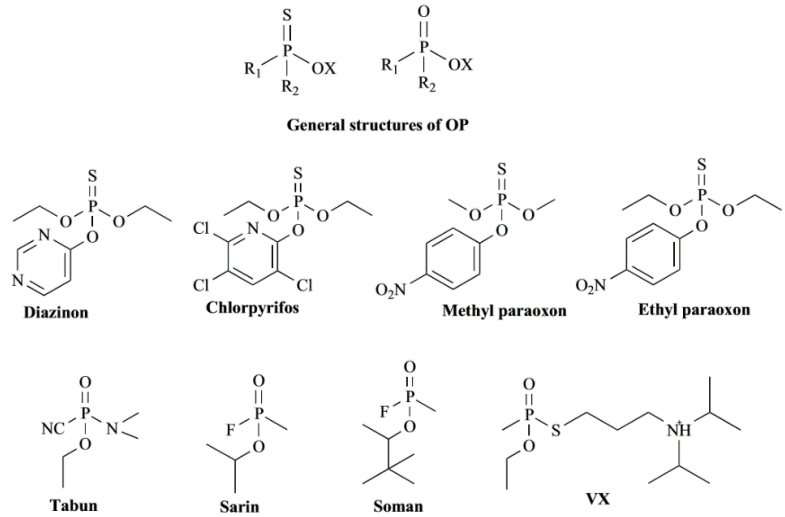

Fig. 13. General structures of organophosphorus (OPs) and common used OP compounds.

This reported knowledge point out that, at the AChE active site, the catalytic triad (Ser203-Glu334-His447) is found at the bottom of the active site gorge, surrounded by three important structural features for catalytic activity: the acyl pocket (residues Phe295, Phe297 and Phe338), the oxyanion hole (main chain nitrogen from residues Gly121, Gly122 and Ala204), and the choline-binding site (Trp86 and Tyr337) (**Fig A**). The phosphoryl oxygen of tabun adduct interacts with the amino acid residues in the oxyanion hole (distance of 2.5, 2.7 and 3.0Å from Gly121, Gly122 and Ala204, respectively). The dimethylamino group is in the acyl pocket, interacting with Trp236 and Phe338 residues (**Fig B**). The two Zn^{2+} ions (α-Zn and β-Zn) in the PTE active site are found at a distance of ~3.4Å from each other and they are linked to the enzyme structure by means of the side chains of His55, His57, His201, His230, Asp301 and Lys169. (**Fig C**).

The proposed reaction mechanism for the PTE catalyzed reaction begins with a nucleophilic attack by an activated water molecule on the P center, resulting in an inversion of configuration. That is, the reaction takes place via bimolecular nucleophilic substitution (SN2) mechanism, where the Asp301 serves as a weak base, which removes an H atom of the water molecule, activating it. Afterwards, the resulting hydroxyl ion attacks the central P. A second reaction mechanism is possible

for the OP degradation by PTE. In this case, there will be an attack to the P center directly by the carboxylic oxygen from the side chain of Asp301, promoting the expulsion of the leaving group and

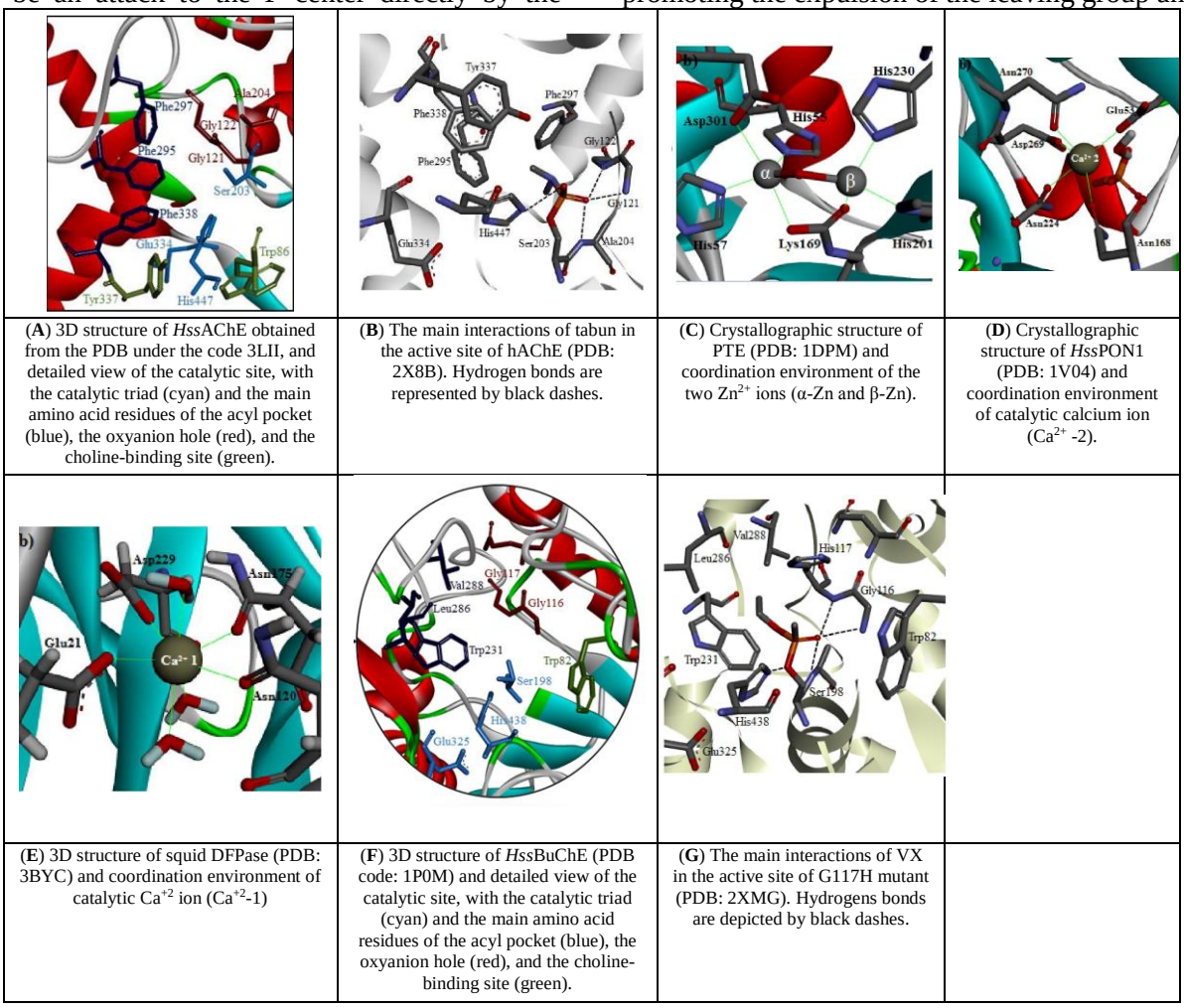

(**A**) 3D structure of *Hss*AChE obtained from the PDB under the code 3LII, and detailed view of the catalytic site, with the catalytic triad (cyan) and the main amino acid residues of the acyl pocket (blue), the oxyanion hole (red), and the choline-binding site (green).

(**B**) The main interactions of tabun in the active site of hAChE (PDB: 2X8B). Hydrogen bonds are represented by black dashes.

(**C**) Crystallographic structure of PTE (PDB: 1DPM) and coordination environment of the two Zn^{2+} ions (α-Zn and β-Zn).

(**D**) Crystallographic structure of *Hss*PON1 (PDB: 1V04) and coordination environment of catalytic calcium ion (Ca^{2+} -2).

(**E**) 3D structure of squid DFPase (PDB: 3BYC) and coordination environment of catalytic Ca^{+2} ion (Ca^{+2}-1)

(**F**) 3D structure of *Hss*BuChE (PDB code: 1P0M) and detailed view of the catalytic site, with the catalytic triad (cyan) and the main amino acid residues of the acyl pocket (blue), the oxyanion hole (red), and the choline-binding site (green).

(**G**) The main interactions of VX in the active site of G117H mutant (PDB: 2XMG). Hydrogens bonds are depicted by black dashes.

Fig. 14. Detailed view of the catalytic site of OP degrading enzymes with their ligands **[8]**.

cleavage of the OP. This reaction is assisted by Asp301 (for **Fig C**).In the active site f DFPase, the Ca^{+2}-1 is coordinated with seven ligands, three water molecules and the side chain of Glu21, Asn120, Asn175, and Asp229 (**Fig E**).

BuChE has a large active site (500 Å³) and it is normally subdivided in four parts: the acylation site, the choline-binding pocket, the acylbinding pocket and the peripheral anionic site (PAS). The acylation site is located at the bottom of the gorge and contains the catalytic triad: Ser198, Glu325 and His438 in *Hss*BuChE. The oxyanion hole is important to provide stabilization to the proposed transition states in the hydrolysis reaction through H-bonds and it consists of the side chains of residues Gly116, Gly117 and Asp199. The key residue of the choline-binding pocket is the Trp82, which is involved in cation-π interactions. The acyl-binding pocket is composed mainly by Trp231, Leu286 and Val288. And, lastly, the PAS is located at the rim of the gorge, however this is controversial because three key aromatic residues in the PAS of AChE are missing in BuChE (**Fig F**).

Proposed hydrolysis mechanism for *Hss*BuChE cover that as a first Ser198 is activated by His438 and Glu325 and then Ser198 attacks the OP center, forming a pentavalent TS, before the departure of the leaving group. The TS is stabilized by the amino acid residues in the oxyanion hole. Then, a phosphorylated enzyme intermediate is formed. This intermediate is very stable in the wild type *Hss*BuChE but unstable in the G117H mutant. The following step is the nucleophilic attack on the P atom by a water molecule, which may be activated by His438. Lastly, the product is released and the enzyme regenerated (for **Fig F**).

In (**Fig G**), the main interactions of VX in the G117H active site are represented. The VX adduct is positioned in such way that methyl group is located near His438 and the ethoxy group in the acyl-binding pocket, pointing toward Val288. The phosphoryl oxygen is interacting with the main-chain nitrogen atoms of the residues in the oxyanion hole (distance of 2.7, 2.8 and 3.2Å from His117, Gly116 and Ala199, respectively).

As pointed out at the many manuscript, bioremediation presents the most promising technology today to destroy OPs have been shown to be very efficient in detoxification of several OPs but the lack of knowledge of their mechanisms of action have limited the development of this action of these enzymes and have already contributed to important advances in the engineering of more efficient OP degrading enzymes. It is apparent that the theoretical investigations will continue reveal much more and contribute for the development of more efficient ways of detoxifying OPs **[8]**.

On the other hand, our focused on spesific functional heterocycle, 2-iminothiazoles are designed, synthesized and tested as protein tyrosine phosphatase 1B inhibitors **[9]**, cannabinoid receptor ligands **[7]**, pifithrin-α p53 inactivators **[10]**, etc. there is not any remarkably record on their insecticidal docking study.

technology. Fortunately, computational enzymology, using molecular modeling techniques like molecular docking, MD simulations, and QM/MM studies, provide the appropriate tools to improve the knowledge of the mechanisms of

The present work aimed to introduce the molecular modelling and mapping of active site of previously synthesized by us insectisidal 2-iminothiazole derivatives **[11]**, by using classical docking techniques, *i.e.* MOE, etc. **[12]**

2. MATERIAL AND METHODS

Synthesis

Synthetic procedure of 2-iminothiazole compounds was described previously by us **[11]**. Promising insecticid derivatives were selected for docking data set and illustrated on Table 1.

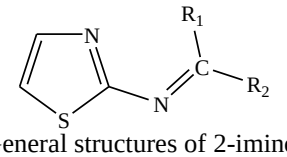

Fig. 15. General structures of 2-iminothiazoles

Table 1. The structures of tested compounds:

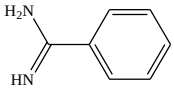

Benzamidine

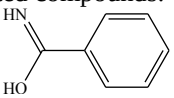

Benzimidic acid

Tested comp. ID	The structures of tested compounds	Tested comp. ID	The structures of tested compounds	Tested comp. ID	The structures of tested compounds
6	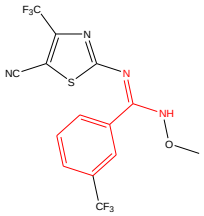 N-(5-Cyano-4-trifluoromethyl-thiazol-2-yl)-N'-methoxy-3-trifluoromethyl-benzamidine	9	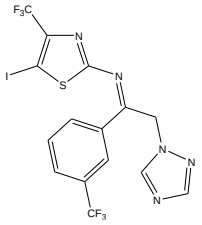 (5-Iodo-4-trifluoromethyl-thiazol-2-yl)-[2-[1,2,4]triazol-1-yl-1-(3-trifluoromethyl-phenyl)-ethylidene]-amine	26	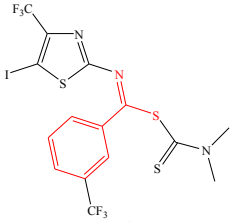 N-(5-Iodo-4-trifluoromethyl-thiazol-2-yl)-3-trifluoromethyl-thiobenzimidic acid dimethyldithiocarbamyl ester
95	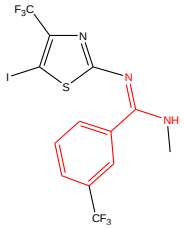 N-(5-Iodo-4-trifluoromethyl-thiazol-2-yl)-N'-methyl-3-trifluoromethyl-benzamidine	98	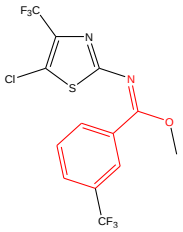 N-(5-Chloro-4-trifluoromethyl-thiazol-2-yl)-3-trifluoromethyl-benzimidic acid methyl ester	99	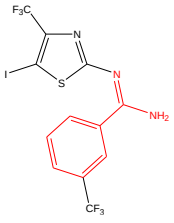 N-(5-Iodo-4-trifluoromethyl-thiazol-2-yl)-3-trifluoromethyl-benzamidine

121

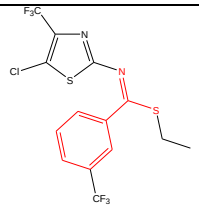

N-(5-Chloro-4-trifluoromethyl-thiazol-2-yl)-3-trifluoromethyl-thiobenzimidic acid ethyl ester

143

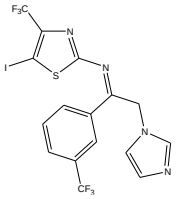

[2-Imidazol-1-yl-1-(3-trifluoromethyl-phenyl)-ethylidene]-(5-iodo-4-trifluoromethyl-thiazol-2-yl)-amine

Materials

Literature search were performed by using SciFinder, Web of Science and Protein Data Bank databases. Chemical drawing programs: 2D Drawings were made using ChemDraw and ISIS Draw programs. 3D drawing of chemical molecules was carried out using the MOE 2016 program (AUBAP, 2017, 1701S009). All text writing and chemical drawing, application procedure were accomplished by Intel Core i7 processor (7700 HQ), Windows 2010 operating system workstation (AUBAP, 2017, 1701S009). For docking study, reference ligand-receptor/protein complexes were transferred from RCSB Protein Data Bank for known active site placement. For docking study, the active chemical compound (ligand) was removed from the ligand-receptor/protein complex crystal which is transferred from the Protein Data Bank, and replaced with designed compounds, then investigate to whether show similar interactions with the reference ligand.

Methods

As initial, data set compounds overlay and observed the alignments. As a first attempt to docking, imidacloprid (IMI) was selected as model and its crystal complex structure with nicotinic acetilcholine receptor (nAChRs) was retrieved from the RCSB Protein Data bank (PDB: 2ZJ**U**).

Molecular docking

Preparation of receptor

Molecular Operating Environment (MOE 2016) was used for current studies **[12]**. The protein preparation step involved 3D protonation energy minimization and active site identification. The crystal structure of Ls-AChBP was obtained from protein data bank (PDBID 2ZJU) **[2]**. The co-crystallized bound compound and water molecules were stripped off from the crystal structure. Protein was energy minimized and 3-D protonated by using the structure preparation module of MOE. As the protein contains the co-crystallized ligand, the active site was identified by using site finder module of the MOE. The pocket was found to be deep cleft lined with the key residues including both hydrophobic and hydrophilic amino acids.

Preparation of ligands

The ligand files for molecular docking studies were prepared in Molecular Operating Environment (MOE-2016.0802) by chemical computing group (CCG) and were followed by energy optimization at standard MMFF94 force field level, with a 0.0001 kcal/mol energy gradient convergence criterion **[12]**. The optimized geometries were saved in molecular data base file for further studies.

Molecular docking studies

The optimized ligands were docked with the Ls-AChBP (PDBID 2ZJU) protein using the MOE-Dock program. For docking, default MOE docking parameters, i.e. Triangle Matcher Algorithm with two rescoring functions, London dG and GBVI/WSA dG were utilized to generate 30 poses of each compound. As a result of docking run, mdb output files were generated enclosing all docking results with scoring and multiple conformations of ligands. All the docked conformations were analyzed and the best scored pose for each compound was selected for further studies of interaction evaluation. The 2D ligand-protein interactions were visualized using the MOE ligand interactions program.

RESULTS

Activity on nicotinic acetilcholine receptors (nAChRs) has been checked by using Ls-AchBP crystal structure complexed with imidacloprid (PDBID 2ZJU) replaced by data set. Docked compounds on 2ZJU showed correspondence interaction with imidacloprid.

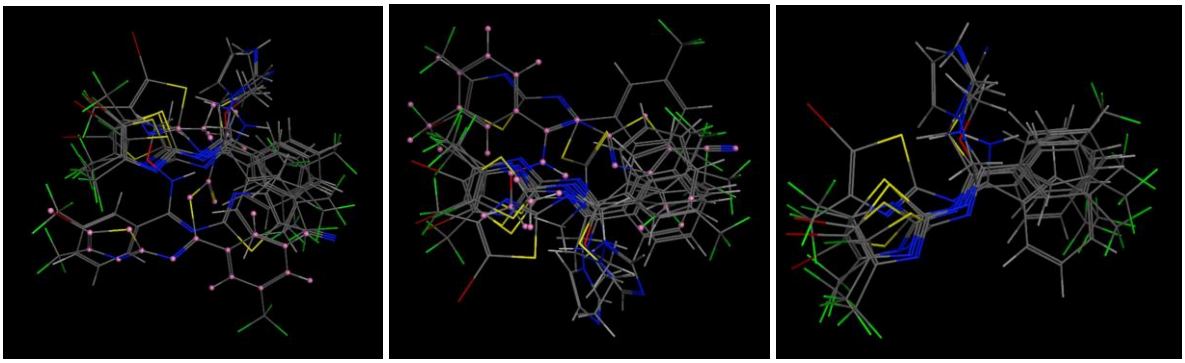

Fig. 16. Alignment of dataset compounds. (a) Selected compound as pink is Comp. 26;(b) Selected compound as pink is Comp. 6; (c) Alignment of all dataset compounds except Comp. 26 and Comp. 6.

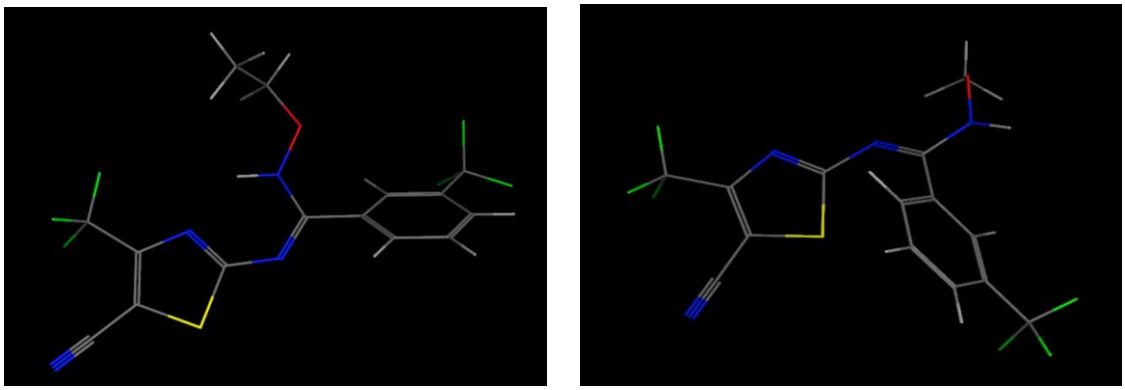

Fig. 17. Two possible configuration of Comp. 6.

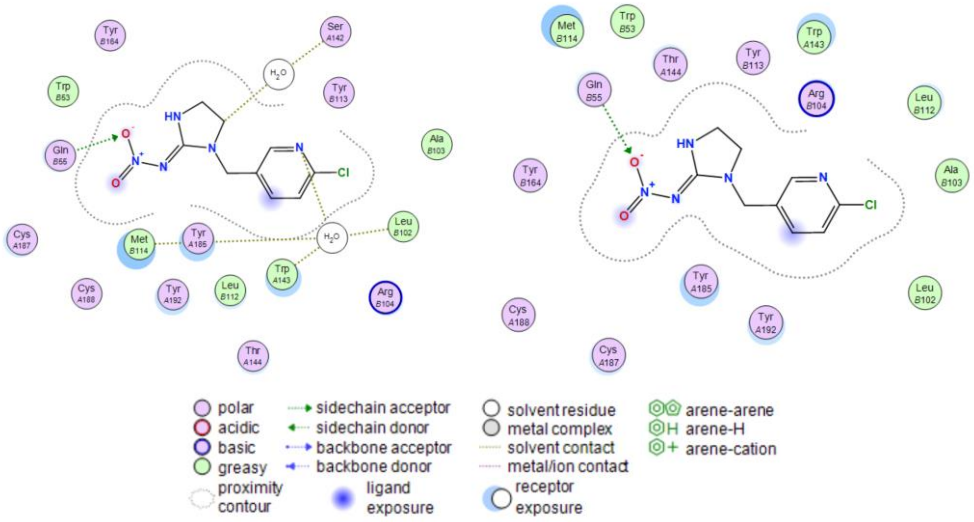

Fig. 18. PDB: 2ZJU ligand interaction with its own ligand IMI **(a)** together with water, **(b)** later than removed water.

CONCLUSIONS

It is stand out that the alignment of data set is not able to accomplish because of non-symmetric property of imines. Their configuration of imines may result in different activity or ranging from more to less affinity to related enzyme binding. To identify clearance of activity, further purification and elucidation of structures i.e. X-ray crystallography may offer valuable activity results for non-symmetric imines. Based on the preliminary docking study of data set, we observed favourable interaction complexes of the designed compounds with target protein Ls-AchBP. Further biological testing will be carried out to verify the docking studies. In accordance with the *in-silico* docking and activity results would allow us to develop new strategies for novel active compounds.

Acknowledgements. *This work is partly supported by Anadolu University, Scientific Research Projects Commission, 2017, Project Number ≠1701S009.*

REFERENCES

1.https://products.basf.com/documents/pim;view/en/879746.5586133.Insecticide%20Mode%20of%20Action%20Technical%20Training%20Manual.pdf
2. M. Ihara, T. Okajima, A. Yamashita, T. Oda, K. Hirata, H. Nishiwaki, T. Morimoto, M. Akamatsu, Y. Ashikawa, S. Kuroda, R. Mega, S. Kuramitsu, D.B. Sattelle, K. Matsuda, *Invert. Neurosci*., **8,** 71 (2008).
3. M. Suganthi, K.P. Elango, *Phys. Chem. Liq.*, **55,** 165 (2017).
4. A.C.V. Martins, F.W.P. Ribeiro, G. Zanatta, V.N. Freire, S. Morais, P. Lima-Neto, A.N. Correia, *Bioelectrochemistry*, **108**, 46 (2016).
5. R.R.K. Niraj, V. Saini, A. Kumar, *Env. Toxic. Pharm*., **40,** 886 (2015).
6. T.-T. Yao, J.-L. Cheng, B.-R. Xu, M.-Z. Zhang, Y.-Z. Hu, J.-H. Zhao, X.-W. Dong, *RSC Advances*, **5**, 49195 (2015).
7. W.A. Carroll, M.J. Dart, A. Perez-Medrano, J.M. Frost, S. Peddi, *US Patent* 20080287510 A1 (2008).
8. T.C. Ramalho, A.A. Castro, D.R. Silva, M.C. Silva, T.C.C. Franca, B.J. Bennion, K. Kuca, *Cur. Med. Chem*., **23,** 1041 (2016).
9. D.-R. Ahn, J. Lee, D. Shin, *Bull. Korean Chem. Soc*., **34,** 2861 (2013).
10. N. Pietrancosta, F. Maina, R. Dono, A. Moumen, C. Garino, Y. Laras, S. Burlet, G. Quelever, J.-L. Kraus, *Bioorg. Med. Chem. Lett*., **15,** 1561 (2005).
11. I. Iwataki, A. Meriç, E.L. Moyano, R. Hatano, *US Patent 6 617 341 B1* (2003).
12. https://www.chemcomp.com/MOE2016.htm